

Kinetic Model of Stage Transformation and Intercalation in Graphite

P. Hawrylak^(a) and K. R. Subbaswamy^(b)

Department of Physics and Astronomy, University of Kentucky, Lexington, Kentucky 40506

(Received 15 June 1984)

We derive a set of diffusion equations based on time-dependent Landau-Ginzburg theory, which is capable of describing the role of domains in stage transformations and intercalation in layered materials. As illustrations of the formalism we study stage decomposition in a quenched sample and the intercalation of a dilute sample. Staggered domains of intermediate stages are shown to arise naturally as a consequence of the interactions and the kinetic constraints even for a sample without dislocations. Further, we show that intercalation proceeds through the formation and migration of islands of intermediate stages.

PACS numbers: 61.60.+m, 64.60.My, 64.70.Kb

The important role of domains in the physics of graphite intercalation compounds¹ has been underscored in recent experimental and theoretical work. The domain model of Daumas and Herold² (DH) assumes that in a staged sample (stage n refers to a periodic sequence of intercalant layers separated by n carbon layers) the areal density of intercalants is the same for every carbon layer (averaged over the whole sample) so that there are staggered domains of pure stage material. The DH model has been invoked to explain qualitatively the mechanism of stage transformations,²⁻⁴ stage disorder,⁵ and other processes.^{6,7}

In the description of all the above phenomena the existence of intercalant domains is taken for granted, and equilibrium thermodynamics is used. While various models⁸⁻¹¹ for the phase diagram of the homogeneous system have been constructed, no related theory of the kinetics of stage transformation and intercalation involving the inhomogeneous

DH structures exists. The purpose of the present paper is to point out that apart from the formation of domains by nucleation of dislocations¹² the interactions responsible for staging and the kinetic constraints appropriate to lamellar structure lead naturally to an intrinsic tendency to form DH structures. The fact that the various staging-related phenomena are observed in single crystal as well as highly oriented pyrolytic graphite suggests that this intrinsic effect might also play a significant role in the physics of intercalation. Our approach is based on the theory of spinodal decomposition^{13,14} considered in this context first by Safran¹⁵ to study the dynamics of domain growth.

We start with a mean-field lattice-gas model of staging as proposed by Safran.⁸ Consider a system of N carbon layers stacked along the z axis. Let $\sigma_j(x,y)$ be the coarse-grained intercalant density on the j th layer normalized to unity for close-packed density. The total Helmholtz free energy of the system may be written as

$$F = \int \int dx dy \sum_j [F_j + \frac{1}{2}\kappa(\nabla_{x,y}\sigma_j)^2 + \sum_{i>j} \sigma_j V_{ij}\sigma_i]. \quad (1)$$

The first term is the free-energy density of a single layer which we take to be

$$F_j = -\frac{1}{2}U_0\sigma_j^2 + k_B T[\sigma_j \ln \sigma_j + (1-\sigma_j)\ln(1-\sigma_j)] + \gamma\sigma_j/(\beta + \sigma_j). \quad (2)$$

The first two terms in Eq. (2) are common to equilibrium models^{8,9} and the third contribution is an elastic energy due to the separation of the layers.¹⁰

The second term in Eq. (1) is the energy-gradient term.^{13,14} It expresses the fact that it costs the system energy to introduce density inhomogeneities along the basal planes; κ determines the interface energy and the size of the islands. The third term in Eq. (1) is the interlayer repulsion¹⁶ which we take to be of the form $V_{ij} = V_0/|i-j|^4$ as has been done in most equilibrium studies.^{8,11} Note that long-range elastic forces which can play an impor-

tant role in island formation¹⁷ have also been left out for simplicity.

The phase diagram for the homogeneous system is obtained in the standard way.⁸⁻¹¹ All our kinetic studies reported here will be with reference to the equilibrium phase diagrams calculated in this manner for the parameters $V_0/U_0=0.3$, $\gamma/U_0=1.05$, and $\beta=0.5$. Estimates for U_0 for intercalated graphite are of the order of 0.25 eV.¹ The resulting phase diagram ($k_B T/U_0$ versus overall intercalant concentration N_I) showing stages 1, 2, 3, and fractional stage $\frac{3}{2}$ (periodic array of stacks of

three carbon layers, with two of them filled) is displayed in Fig. 1 for future reference.

We first study mass-conserving stage transformations such as the quenching process indicated by the dashed line AB in Fig. 1. Note that mass-conserving stage transformations by varying hydrostatic pressure have been studied experimentally.^{4,18} To describe such processes we assume that the intercalant density on every layer is conserved. This is reasonable since in a perfect crystalline sample diffusion across the graphite layers is highly improbable in light of the relative ion sizes. The intercalant flux on the i th layer is linearly related to the thermodynamic force, i.e., the gradient of the local chemical potential¹⁴:

$$\vec{J}_i = -M \nabla_{x,y} \mu_i, \quad (3)$$

where $\mu_i = \delta F / \delta \sigma_i$ and F is given in Eq. (1), and M is the mobility (assumed constant). Since the layer occupancy is conserved, we have the equation of continuity¹⁴

$$\partial \sigma_i / \partial t = -\nabla_{x,y} \cdot \vec{J}_i. \quad (4)$$

Equations (1)–(4) describe the time evolution of the system for mass-conserving processes. These coupled, nonlinear diffusion equations constitute our kinetic model. We will show below that they can be adopted for describing the intercalation pro-

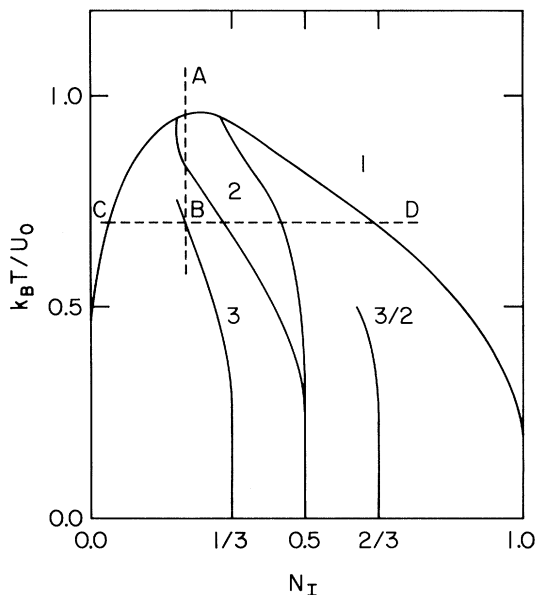


FIG. 1. The equilibrium phase diagram for the free-energy model under consideration. N_I is the overall intercalant concentration. The kinetics of the processes indicated by the dashed lines AB and CD are considered as illustrations here.

cess as well under some simplifying assumptions.

We now apply the above model to study the kinetics of the stage decomposition resulting from the quench represented by the dashed line AB in Fig. 1. Our initial configuration corresponds to that of high-temperature stage 1, i.e., a uniform occupancy of $\sigma_0 = 0.225$ on every layer, which corresponds to the equilibrium configuration for this concentration at $\tilde{T} (= k_B T / U_0) = 1.1$. The system is quenched to temperature $\tilde{T} = 0.7$ for which a stage-3 configuration (in-plane occupancies of 0.625, 0.025, and 0.025 on successive layers) is the equilibrium configuration if the system is homogeneous. A linear stability analysis¹⁹ with respect to basal-plane sinusoidal density fluctuations with z -axis periodicities 1, 2, and 3 shows that the fastest growing instability is of periodicity 2, i.e., that of stage-2 type. This would imply that a sample quenched directly from high-temperature stage 1 to the region of stability of stage 3 must pass through an intermediate phase with stage-2 domains. The linear stability analysis yields the critical (Cahn-Hilliard)¹³ wave vectors at which the fastest growing mode of instability occurs (stage-2 type) to be $\sim 0.35\pi / \sqrt{\kappa}$. For the temperatures under consideration here the value of $\sqrt{\kappa}$ should be of the order of $\sim 20 \text{ \AA}$, so that the decomposition wavelength is of the order of 120 \AA . The initial growth rate is of the order of κ / MU_0 which we estimate (from the reported diffusion rates²⁰) to be of the order of 10^{-6} s .

As a first step in studying the full effect of the nonlinearity of the diffusion equations we have integrated them for a system of six layers with the concentration assumed to be independent of the y direction. This forces the decomposition to occur through striped domains rather than droplets as in a real system. Because of the in-plane isotropy the qualitative aspects of the early stage decomposition are unaffected by this restriction (e.g., the linear stability analysis still yields stage 2 as the fastest growing mode again), but the late stage-coarsening kinetics in the real system will be much slower. The integration is performed by making the layers discrete along the x direction, where we have chosen 24 points with a lattice constant equal to $\sqrt{\kappa}$ ($\sim 20 \text{ \AA}$) with periodic boundary conditions in the x and z directions. We have verified that with our choice of lattice spacing and chain length the decomposition wavelength agrees well with the Cahn-Hilliard value.

The result for the quenching process AB is shown in Fig. 2(a). Density profiles for the six layers are shown at $t = 10$ and $t = 200$ (measured in units of

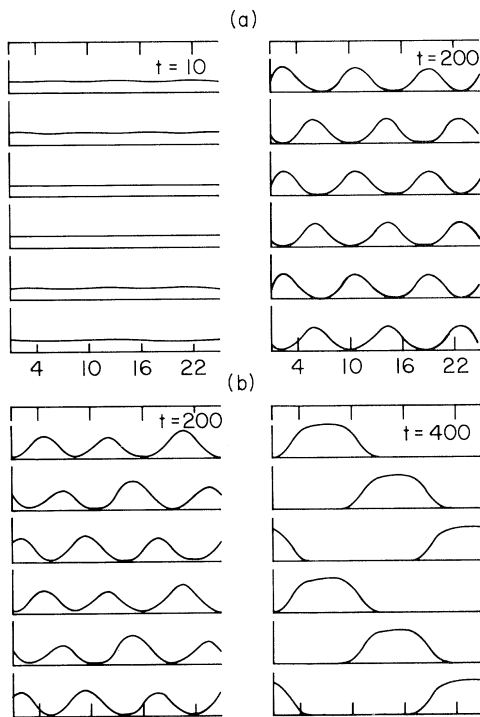


FIG. 2. Density profiles for the quenching process for the six layers at various times. Distance is measured in units of $\sqrt{\kappa}$ ($\sim 20 \text{ \AA}$) and times in units of κ/MU_0 ($\sim 10^{-6} \text{ s}$). (a) The approach to the stage-2 DH stationary (metastable) configuration. (b) The approach to the stage-3 DH configuration.

κ/MU_0 , which is of the order of 10^{-6} s for the parameters here). The initial uniform stage-1 configuration is unstable so that any arbitrarily small perturbation of any kind will lead to the stage-2 mode as predicted by linear stability analysis and verified explicitly here. The next process to be expected is the growth of stage-2 domains to reduce interfacial energy, followed by rediffusion to form stage-3 DH domains. However, we find that the configuration shown for $t=200$ in Fig. 2(a) is a stationary solution stable against small perturbations, and thus represents a metastable state for the system. From the similarity of the stability analyses for the stripe and the droplet cases we believe that this behavior will be true for the two-dimensional simulation as well. If our equations contained a stochastic force term (representing interaction with a thermal bath) the stable stage-3 structure would be reached eventually. The same effect can be illustrated by suppressing the growth of stage-2 fluctuations as shown in Fig. 2(b). Here, the $t=200$ configuration corresponds to one obtained by a three-layer simulation and repeated. Starting with this

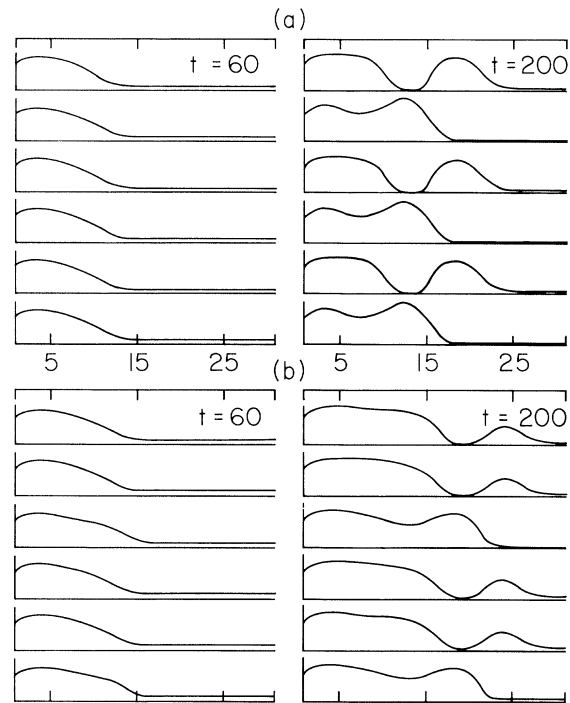


FIG. 3. Density profiles for the intercalation process for the six layers at various times (distance and time units same as in Fig. 2). (a) Formation of stage-2 islands. (b) Formation of stage-3 and stage- $\frac{3}{2}$ configurations.

configuration, the six-layer simulation yields the stage-3 DH structure shown at $t=400$ which has lower free energy (as verified explicitly). Thus, the passage of the system from the high-temperature phase to the low-temperature phase occurs through intermediate stages, which may persist for long times.

Turning now to the intercalation process itself, we consider the simplest possible model of the graphite-vapor interface. Some of these simplifications can be relaxed at the cost of additional computational effort. We will neglect the effect of the sample edges on the interactions, the effect of the finite thickness, and the effect of the c face. The sample is in contact with the vapor on the planes $x = \pm L$ so that the intercalation front is uniform in the y direction. We assume the intercalation to proceed isothermally. Then, the difference in the chemical potential of the intercalant in the graphite matrix and that in the vapor phase drives the intercalation or the deintercalation process until equilibrium is reached. From our simplifying assumptions the evolution equations are unchanged, except for the points on the planes $x = \pm L$. At these points the incoming flux is determined by the difference

between the local chemical potential and the vapor-phase chemical potential.

As an illustration of the scheme we consider the intercalation process indicated by the dashed line *CD* in the phase diagram of Fig. 1. This corresponds to the passage of the sample from a very dilute stage-1 configuration (in-plane occupancy of ~ 0.033) at $\tilde{T}=0.7$ and $\mu=0.35U_0$ to a dense stage-1 configuration at the same temperature and $\mu=1.0U_0$ (in-plane occupancy of 0.755) with mass uptake. We have integrated the diffusion equations for a system of six layers with periodic boundary conditions in the *z* direction with a length along the *x* axis of $72\sqrt{\kappa}$ (with $\sqrt{\kappa}\sim 20\text{ \AA}$ as before) and assuming symmetry with respect to $\pm x$. If the starting configuration is completely homogeneous, the intercalation front would also be homogeneous, though unstable. Introducing small inhomogeneities at the interface then leads to the breaking up of the intercalation front. The results for two separate runs are shown in Fig. 3. In Fig. 3(a), where the initial inhomogeneity was a small excess on the first layer at the interface, the configuration at $t=200$ shows a sample which has attained the high-density stage-1 configuration at the edges, while in the bulk of the sample the intercalant propagates through stage-2 staggered islands. In Fig. 3(b), where the initial inhomogeneity was a stage-3 nucleus at the interface, the intercalation front breaks up into stage-3 and stage- $\frac{3}{2}$ regions. The rate of intercalation found here is compatible with observed rates. Our simulation results support the view²¹ that intercalation proceeds through the growth of domains correlated along the *c* direction due to the repulsive interplane interaction.

In conclusion, we have extended the equilibrium models of intercalation compounds to study time-dependent, kinetic processes. We show that the models predict spinodal-type instabilities which should be observable in carefully controlled quench experiments. In our illustrative examples the occurrence of Daumas-Herold domains is indicated.

This research was supported in part by the National Science Foundation through Grant No.

DMR-8216212.

^(a)Present address: Department of Physics, Brown University, Providence, R.I. 02912.

^(b)Address until March 1985: International Centre for Theoretical Physics, I-34100 Trieste, Italy.

¹M. S. Dresselhaus, *Phys. Today* **37** (3), 60 (1984); *Proceedings of the Third Conference on Intercalation of Compounds of Graphite*, *Synth. Met.* **7** and **8** (1983).

²N. Daumas and A. Herold, *C. R. Acad. Sci., Ser. C* **268**, 273 (1969).

³R. Clarke, N. Caswell, and S. A. Solin, *Phys. Rev. Lett.* **42**, 61 (1979).

⁴R. Clarke, N. Wada, and S. A. Solin, *Phys. Rev. Lett.* **44**, 1616 (1980).

⁵G. Kirczenow, *Phys. Rev. Lett.* **52**, 437 (1984).

⁶G. Forgacs and G. Uiman, *Phys. Rev. Lett.* **52**, 437 (1984).

⁷G. Schoppen, H. Meyer-Spasche, L. Siemgluss, and W. Metz, *Mater. Sci. Eng.* **31**, 115 (1977).

⁸S. A. Safran, *Phys. Rev. Lett.* **44**, 937 (1980).

⁹S. Millman and G. Kirczenow, *Phys. Rev. B* **26**, 2310 (1982).

¹⁰J. R. Dahn, D. C. Dahn, and R. R. Haering, *Solid State Commun.* **42**, 179 (1982).

¹¹P. Hawrylak and K. R. Subbaswamy, *Phys. Rev. B* **28**, 4851 (1983).

¹²J. M. Thomas, G. R. Milward, R. F. Schlogl, and H. P. Boehm, *Mater. Res. Bull.* **15**, 671 (1980).

¹³J. W. Cahn and J. E. Hilliard, *J. Chem. Phys.* **28**, 258 (1958).

¹⁴J. S. Langer, in *Fluctuations, Instabilities and Phase Transitions*, edited by T. Riste, NATO Advanced Study Institute Series B, Vol. 11 (Plenum, New York, 1975), p. 19.

¹⁵S. A. Safran, *Synth. Met.* **2**, 1 (1980).

¹⁶S. A. Safran and D. R. Hamann, *Phys. Rev. B* **22**, 606 (1980).

¹⁷S. A. Safran and D. R. Hamann, *Physica (Utrecht)* **99B**, 469 (1980).

¹⁸C. D. Fuerst, J. E. Fischer, J. D. Axe, J. B. Hastings, and D. B. McWhan, *Phys. Rev. Lett.* **50**, 357 (1983).

¹⁹P. Hawrylak, Ph.D. dissertation, University of Kentucky, 1984 (unpublished).

²⁰A. Magerl, H. Zabel, J. J. Rush, and A. J. Dianoux, *Synth. Met.* **7**, 227 (1983).

²¹D. Kaluarachchi and R. F. Frindt, *Phys. Rev. B* **28**, 3663 (1983).